

3-D Compounding of B-Scan Ultrasound Images

Jochen F. Krücker, Charles R. Meyer, Theresa A. Tuthill, Gerald L. LeCarpentier,
J. Brian Fowlkes, Paul L. Carson

University of Michigan, Dept. of Radiology, 200 Zina Pitcher Place *Ann Arbor, MI 48109, USA*

Summary: Two applications of volume registration in 3-D ultrasound imaging, extended volume imaging (EVI) and 3-D Spatial compounding, are demonstrated both in phantom and clinical scans. Extended volumes were composed by obtaining partly overlapping scans, registering the overlapping volumes, and displaying the complete set of volumes in their relative spatial orientations as determined by the registration procedure. 3-D compound images were created by scanning volumes from several elevational look directions, registering, and averaging the different views. In both applications, the volume registration worked accurately and provided significant image improvements.

INTRODUCTION

Image registration, or coregistration, can be used to combine several sets of images obtained with different imaging parameters or modalities, from different look directions, or at different times. In medical imaging, it has mainly been applied to magnetic resonance imaging, X-ray computed tomography, and tomographic nuclear imaging modalities. Recently it has been shown that some image registration techniques can also be used to register 3-D ultrasound data sets [1-3]. In this study, we demonstrate two registration-based examples of image enhancements in 3-D ultrasound: Extended volume imaging (EVI) and 3-D spatial compounding. With EVI, one of the major limitations of high-frequency ultrasound scanners, the small field of view, can be overcome. This application is particularly important in sequential ultrasound exams, e.g. in screening for breast cancer or following cancer therapy, where large fields of view are needed to locate areas of change and to make sure that the same area is covered in sequential scans. Spatial compounding can deliver improved images with reduced speckle noise and increased contrast-to-noise ratio. It also reduces shadowing, and creates more complete images of connective tissues and other specular reflectors.

MATERIALS AND METHODS

Since the registration algorithm we used is fully explained in [4], we will only briefly describe the relevant features here. The software performs either affine, i.e. linear, geometric transformations to map one image volume onto another, or non-linear thin-plate spline (TPS) warpings. When using full affine transformations, the user places 4 initial control points in each data set. The control points define the approximate mapping transformation from one set (reference) onto another (homologous). By varying the position of the control points, the algorithm refines the transformation until the mutual information (MI) of the reference and the

transformed homologous set is maximized. The MI, defined as the difference between the sum of the individual entropies and the joint entropy of two random variables, thus serves as a cost function in this optimization problem. For warping transformations, the user defines at least one more control point and increases the degrees of freedom of the registration transformation with each additional control point. Note that no pre-processing, like cropping or speckle reduction, has to be applied to the image sets before registration.

A clinical ultrasound scanner (Logiq 700, GE Medical Systems, Milwaukee, Wis) with an 11MHz 1.5-dimensional linear matrix array probe was used for all data acquisition. With electronic elevational (normal to scan plane) focussing, the average axial and elevational resolution cell diameters were 0.31 mm and 0.72 mm, respectively¹. The transducer was attached to a 2 degree of freedom position encoder that restrained the motion of the probe to linear elevational scanning and elevational tilting. The position information was used to uniformly interpolate and shear the raw B-scan image sets before volume registration. All phantom scans were obtained in a focal lesion phantom (CIRS; Computerized Imaging Reference Systems, Norfolk, Va). All clinical scans were obtained in the female breast.

To create extended volume images, the area of interest was imaged in 3 or 4 approximately parallel, partly overlapping scans (Fig. 1). If 3 scans were used, the central scan (B) served as a reference relative to which the outer scans (A, C) were registered by maximization of the mutual information in the overlaps, AB and BC. In cases where 4 scans were combined (A, B, C, and D), D was first registered relative to C. The combined volume (C&D) and volume A were then registered relative to the global reference B using the overlaps BC and AB.

EVI was obtained both in phantom scans and clinical breast scans. In phantom scans, the registration accuracy in the extended lateral direction was evaluated by comparing the true position of 50 spheres (3mm diameter) in the phantom to the position found in the extended view. In clinical scans, the registered volumes were visually assessed and the position of common landmarks marked in each set. The average registration error was defined as the mean distance between point pairs defining common landmarks.

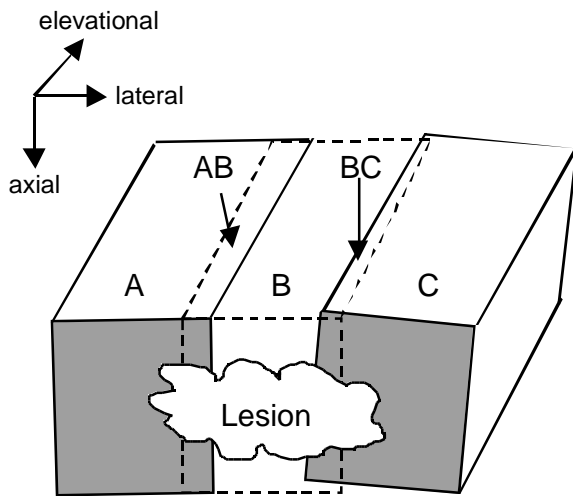


Figure 1: Extended Volume Imaging. Volumes A and C are registered relative to reference volume B.

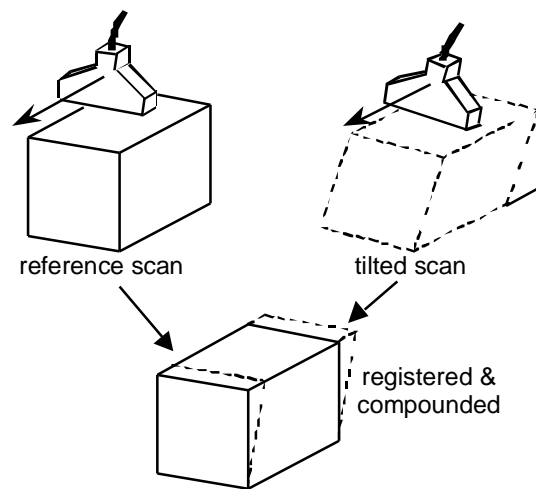


Figure 2: Spatial compounding of volumes obtained at different elevational tilt angles

¹ A phantom was scanned axially and elevationally in an area that produced fully developed speckle. The resolution cell diameters were defined as the standard deviation of the Gaussian fit to the frame-to-frame correlation functions.

For compound imaging, partly uncorrelated views were obtained by changing the tilt angle of the transducer before re-scanning the area of interest (Fig. 2). The interpolated and sheared image sets were registered using either full affine or warping transformations. The registered data sets were then log-decompressed, averaged, and recompressed to the same dynamic range as the original images (69 dB).

The registration accuracy in phantom scans was determined using a semiautomatic edge detection algorithm. Given the approximate center of a spherical hypoechoic area, the algorithm finds the exact center and the two radii on which the average signal increased 10% and 90%, respectively, of the difference between the maximum signal level outside the circle and the minimum inside. The difference between the radii will be referred to as the boundary width of the spheres. The accuracy in clinical compound scans was estimated by the same visual method used for clinical EVI.

RESULTS AND DISCUSSION

Figure 3 displays an example of an axial-lateral cross section through an EVI created from 4 partly (30%, 35%, and 58%) overlapping phantom scans registered with full affine transformations. No averaging or other processing was applied in the areas of overlap. The white arrows indicate the display boundaries between the registered original scans. Note the continuous appearance of specular reflectors across the boundaries and the spherical symmetry of voids placed on boundaries. The total width of the cross section is 10.6 cm. The average lateral deviation of the spheres in the extended volume from their true position is +0.47%.

EVI in clinical scans produced similar alignment quality as long as the breast was stabilized during the scans to keep local tissue deformation at a minimum [5]. The average distance of common landmarks identified in the registered overlaps ranged from 0.8 mm to 1.4 mm (peak: 1.5 to 3.1 mm).

Correlation calculations in phantom scans showed that the change in tilt angle needed to create uncorrelated images is 4 to 6 degrees. In compounding phantom scans obtained at differential scan angles of 4 degrees, the signal-to-speckle noise ratio (SNR) increased 10% to 20% less than the theoretical N dependence for N compounded, uncorrelated images. The average misregistration in phantom scans using full affine transformations was 0.21 ± 0.02 mm and did not vary significantly with tilt angle. As a result of misregistrations, the average boundary width of the spheres in a phantom image compounded from 5 scans increased 20% compared to the uncompounded image. In the same compound image, the SNR increased 95%.

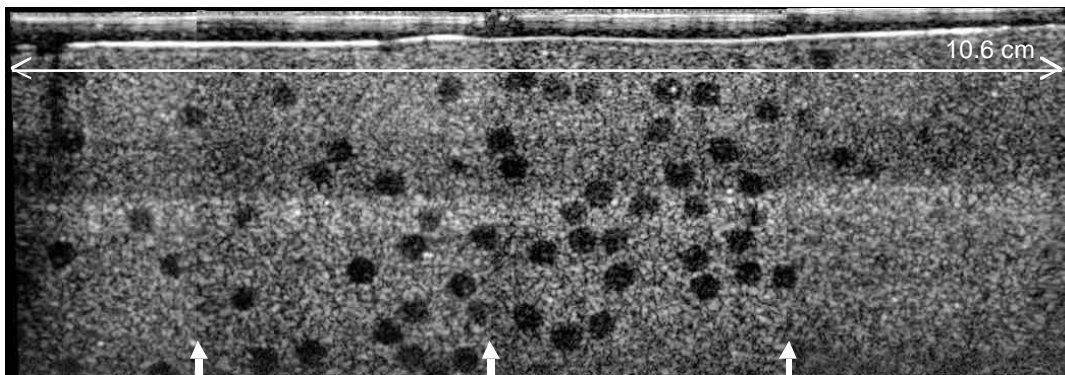


Figure 3: Axial-lateral cross section of an extended volume created from 4 partly overlapping phantom scans.

Figure 4 shows examples of an uncompounded clinical image in breast (a, c), and the same images compounded from 5 scans at 0° , 6.4° , 12.8° , -5.1° , and -10.2° , using 11 control point warping transformations (b, d). Statistical analysis showed an almost ideal \sqrt{N} increase in SNR and CNR (contrast-to-noise ratio) for N compounded images. Note the overall reduction in granularity and the better delineation of connective tissues (arrows).

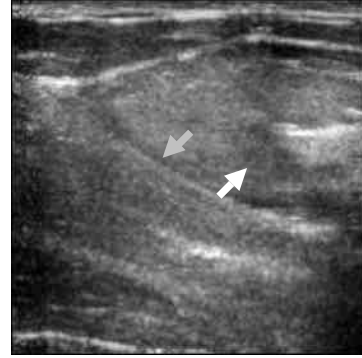


Figure 4: (a) Uncompounded image of a breast from reference, 0° scan. Statistical analysis showed an almost ideal \sqrt{N} increase in SNR and CNR (contrast-to-noise ratio) for N views compounded vs. this reference view. Note the overall reduction in granularity and the better delineation of connective tissues (gray arrow) in (b).

(b) Same image area compounded from 5 scans at 0° , 6.4° , 12.8° , -5.1° , and -10.2° , registered using 11 control point warping transformations. Most importantly, note the slightly hypoechoic, lobulated inhomogeneities surrounding the left end of the hyperechoic structure on the central right. The white arrow denotes one such lobulation with a thin, echogenic rim that is not visible on any of the constituent single views.



(c) Uncompounded image of a breast from reference, 0° scan, 2.4 mm (8 slices) superior to image (a). Structures noted in (d) are not seen as well here.

(d) Same image plane as (c) but from the same compounded image set as (b). Again note the slightly hypoechoic, lobulated inhomogeneities surrounding the left end of the hyperechoic structure on the central right (e.g., white arrows), corresponding to those at the white arrow in (b). Note also the improved delineation of the dark muscle or rib in the lower left (gray arrow) and the tissue striations extending to the right of it.

The same data sets were also registered using full affine transformations. Comparing the warped data sets to the linearly transformed sets we found an increase in average estimated misregistration from 0.42 ± 0.10 mm to 0.75 ± 0.12 mm, suggesting that warping can correct for local tissue deformation that is unaccounted for by global linear transformations.

We conclude that image registration is a promising tool in 3-D ultrasound, allowing applications such as accurate extended volume imaging and 3-D compounding. Using image-based registration with non-linear mapping transformations prior to compounding offers the unique potential to correct for tissue motion and refraction artifacts, effects that can greatly distort image quality in other compounding approaches.

ACKNOWLEDGMENTS

This research was partially supported by U.S. Army Contract No. DAMD17-96-C-6061 and, to a lesser extent, USPHS grant 5RO1CA55076

REFERENCES

1. Meyer, C.R., Boes, J.L., Kim, B., et al., *Ultrasound in Med. & Biol.* (in press)
2. Rohling, R.N., Gee, A.H., Berman, L., *Ultrasound in Med. & Biol.* **24**, pp. 841-854 (1998)
3. Moskalik, A., Carson, P.L., Meyer, C.R., Fowlkes, J.B., Rubin, J.M., Roubidoux, M.A., *Ultrasound in Med. & Biol.* **21**, pp. 769-778 (1995)
4. Meyer, C.R., Boes, J.L., Kim, B., et al., *Med. Image Anal.* **1**, pp. 195-206 (1997)
5. Krücker, J.F., LeCarpentier, G.L., Meyer, C.R., Roubidoux, M.A., Fowlkes, J.B., Carson, P.L., *RSNA Electronic Journal* **3** (1999)